Design and implementation of DC-DC converters for CubeSat in Simulink

Germain Rosadio Vega[a], **Kiara Rodriguez Bautista**[b], **Sheyla Claribel Lozano Burga**[c], **Abad Antialon John Haile**[d], **Omar Enrique Blas Morales**[e]

[a]*National University of Engineering, 15307, +51997813640, grosadiov@uni.pe*
[b]*National University of Engineering, 15018, +51924986997, krodriguezb@uni.pe*
[c]*National University of Engineering, 15018, +51999220421, slozanob@uni.pe*
[d]*National University of Engineering, 15082, +51931274097, john.abad.a@uni.pe*
[e]*National University of Engineering, 15333, +51927966284, oblasm@uni.pe*

Keywords: *CubeSat, EPS, DC-DC Converter, Parameterization*

The present work focuses on the design and simulation of the DC-DC converters used in an Electric Power System (EPS) of a CubeSat through Simulink. The design begins with the sizing of the converter with a set of equations that determine thresholds for the passive components, and whose optimization is studied quantitatively by parameterizing the capacitance and inductance based on the thresholds. The design and parameterization are simulated in LTspice where it is shown that capacitance has an inverse influence on the ripple level, while it slightly increases the efficiency value and has no effect on the overshoot, while inductance increases the efficiency and decreases the overshoot, but does not affect the ripple level. The choice of capacitance and inductance based on the analysis of the characteristic parameters allows an optimization of the boost converter in terms of the ripple level and overshoot of the resulting voltage, and of the working efficiency. We can also get the efficiency curve by parameterizing R and implement it in the DC-DC Converter block in Simulink with an EPS model.

1. Introduction

A CubeSat is a satellite whose manufacturing standard is 1U, which represents a cube with an edge of 10 cm and a mass of up to 1.33 kilograms [1]. Its conceptual development began for the first time in 1999 and was developed for experimental and educational purposes for the university community [2]. The main advantages of a CubeSat are its rapid development, lower manufacturing cost and positioning in orbit. In addition, depending on the start-up period of the project, the needs may vary and this type of satellites are flexible to technology upgrades.

Due to the small size of this satellite, one of the main challenges in its manufacture lies in energy self-sufficiency, that is, having the capacity to generate, store and distribute the electrical energy needed by its components. To meet this objective, it is necessary to design an Electrical Power System (EPS) that can perform all the above mentioned functions; a common EPS is composed of the following subsystems: photovoltaic cells, rechargeable batteries, and a Power Distribution and Conditioning Unit

(PCDU). The photovoltaic cells have the function of supplying electrical energy to the satellite during its orbit when there is incidence of sunlight to charge the battery and keep the other modules operational, they are the main source of energy used in the CubeSat missions [3]. Batteries are intended to store excess energy from the cells and use it when the energy required exceeds the energy they supply, they are considered secondary energy sources and are classified into primary (non-rechargeable) and secondary (rechargeable) batteries. Finally, the PCDU ensures a proper and reliable electrical connection between the power sources and the other modules of the satellite, consisting of a microcontroller, DC-DC converters, a power protection system, sensors, etc.

For proper operation, the EPS of a CubeSat must power an On-board computer, an Automated data control system intended to control the satellite's orientation with respect to the earth, communication receiver and transmitter and payloads as needed.

2. EPS Considerations

2.1. Orbit considered

The importance of taking into account the characteristics of the CubeSat orbit lies in the fact that it mainly influences the irradiation to which the nanosatellite faces will be exposed as well as the external temperature variations it will experience during its orbit; these two aspects affect the performance of the photovoltaic cells and must therefore be considered.

The CubeSat orbit characteristics are considered based on the available data from the MySat-1 nano-satellite project developed by Khalifa University [4, 5, 6], these are summarized in Table 1, while the type of CubeSat motion and orientation is considered according to the nadir pointing scenario [7], which is depicted in Figure 1.

Table 1: MySat-1 orbit characteristics [6]

Parameter	Value
Altitude	450 km
Orbital period (P)	96 min
Illumination time in 1P	60.02 min
Time of darkness in 1P	35.98 min
Start of illumination	727 s
Inclination	51.6°

2.2. CubeSat module power consumption

The CubeSat studied includes the following modules: On-Board Computer (OBC), EPS, Communication Receiver (COM-RX), Communication Transmitter (COM-TX), Attitude Determination and Control System (ADCS), and Payloads. Each of these systems has a certain power consumption and minimum operating voltage in a normal mode and safe mode, these are presented in Table 2. Here it is visualized that in normal mode all modules will be operating regularly, while in safe mode the ADCS and Payload are turned off and the COM-TX module is on for less time, i.e., the satellite transmission time decreases.

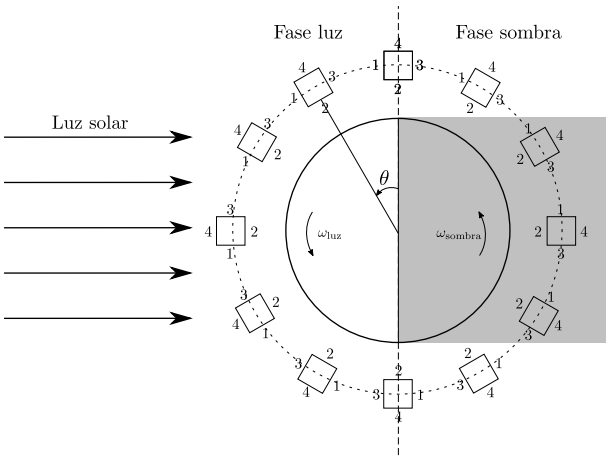

Figure 1: CubeSat path during orbit.

Table 2: CubeSat Power Consumption in normal and safe mode

Module	Power (mW)	Voltage (V)	$t_{ON,normal}$	$t_{ON,safe}$
OBC	400	3.3	1	1
EPS	160	3.3	1	1
COM-RX	480	7.4	1	1
COM-TX	4000	7.4	0.176	0.0667
Camera-Idle	500	5	0.052	—
Camera-Active	1000	5	0.0104	—
ADCS-idle	175	5	0.825	—
ADCS-Active	1200	5	0.176	—

t_{ON}: On-time normalized to orbital period (96 min).

In order to build a power consumption profile of the systems it is also necessary to know their operating modes, such as the instants in which they are activated, and the duration of operation, with this it is possible to build a consumption profile of each system for 1P. The operating time of the systems studied are also presented in Table 2 where the time is normalized with respect to the duration of 1P, and the starting instants are described below:

- The OBC, EPS and COM-RX systems are kept ON during the entire orbit period.
- The Payload system, which is a camera, starts in the OFF state and turns on in idle mode 5 min before the onset of the light phase, where it switches to active mode taking images during 1 min.
- The COM-TX system is turned on right after the Payload finishes operating to transmit its data to an earth station during 16.9 min.
- The ADCS system starts in idle state and at the beginning of the light phase changes to the active state but not in a continuous way, but in the form of pulses, this because it must control the orientation continuously during the light phase if you want a face is fixed to the ground, the total active time is 16.9 min.

The modes of operation of the systems just described result in a total consumed power as in Figure 2, where the gray region represents that the CubeSat is in shadow phase, and in the yellow region in light phase, in addition the total power consumption in normal and safety consumption mode during 1P is presented.

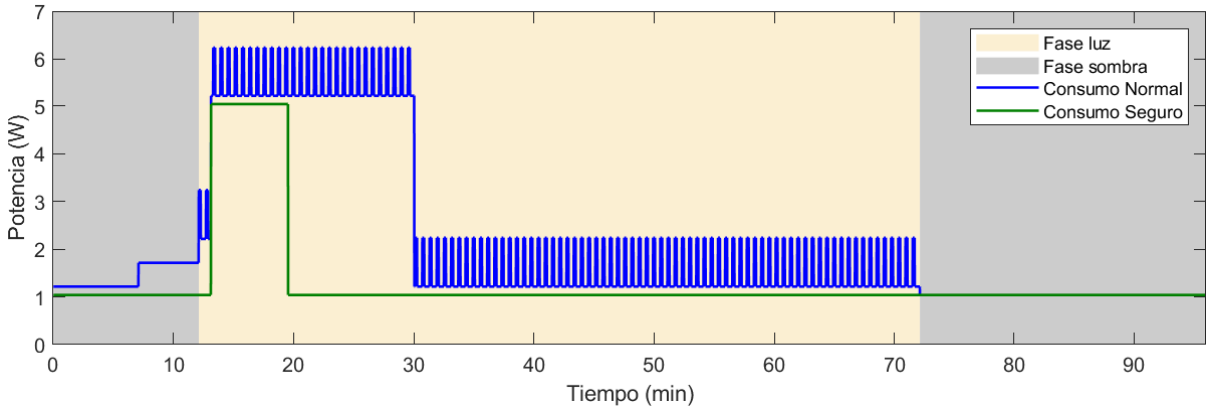

Figure 2: Total power consumption of the loads. In normal mode: P_{min}=1.04 W, P_{max}=6.24 W. In safe mode: P_{min}=1.04 W, P_{max}=5.04 W

3. PCDU Simulink model

The PCDU design is the most customized of the other EPS subsystems since the elements it implements will depend greatly on the mission and requirements, in the work done the PCDU (Figure 3) consists of three DC-DC converters that will adapt the voltage resulting from the cell-battery array to that required by the modules according to the Table 2. It also incorporates a block that will act as a microcontroller evaluating multiple processes during the simulation, this is mainly done by a state diagram.

It is possible to design and simulate a converter such as the boost in Figure 3b in Simulink; however it becomes infeasible to implement in other designs that require very large simulation time because the operating frequency is on the order of kHz (10 kHz [4]). However, Simspace has the block presented in Figure 3b that simulates a DC-DC converter that can be controlled by a voltage signal that will indicate the desired voltage at the output, 5.0 V in the Figure 3b, this block also allows to characterize it with an efficiency curve of a converter, like the one shown in Figure 3c.

The MICRO block contains the state diagram shown in Figure 3d, which has 5 modes of operation of the satellite:

Safety: Safety mode, aims to prevent the battery from being fully discharged. Sending safety mode signal for OBC when SOC decreases from 40%, commanding to start safety consumption.

Batery_dch: Battery discharge mode occurs when the power consumed by the satellite is greater than the power supplied by the cell array, thus the batteries assist the cells in supplying power to the satellite.

Normal_Eclipse: Nominal mode of operation of the EPS when it is in eclipse, where the batteries discharge to supply the satellite's power demand.

Normal_Sol: Nominal mode of operation of the EPS when it is being illuminated by the Sun, where the batteries are recharged and the solar panels supply power to the satellite.

Batery_full: Full battery charge mode occurs when the satellite is being illuminated by the Sun, the battery is at maximum charge (100%) and the cells are supplying power to the satellite.

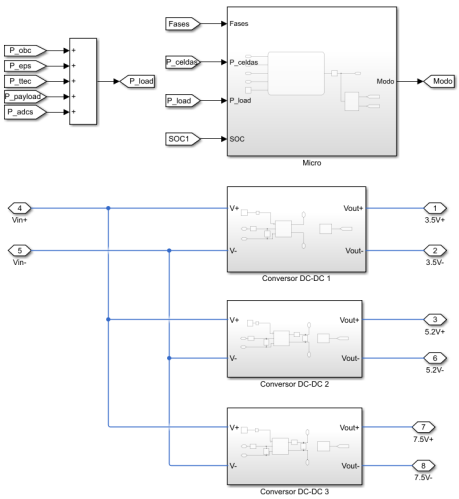

(a) Components of the PCDU.

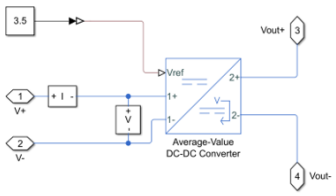

(b) DC-DC converter block

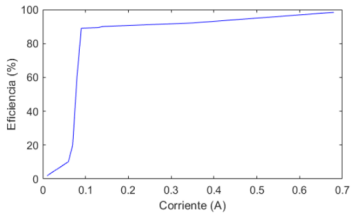

(c) Converter Default Efficiency Curve.

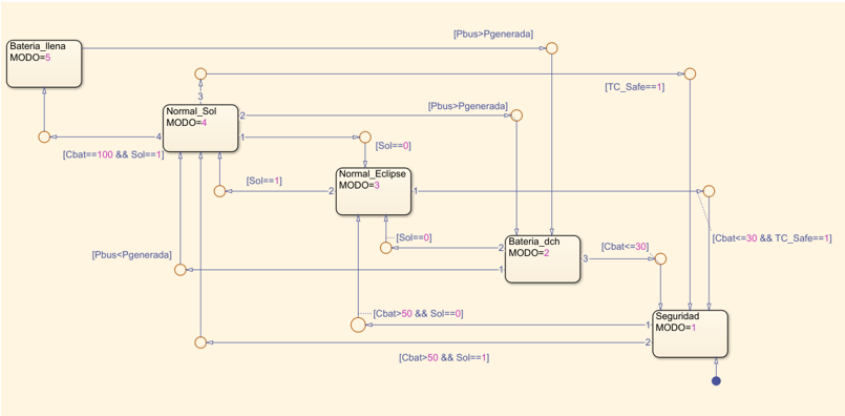

(d) State diagram implemented as microcontroller.

Figure 3: Simulink design of the PCDU implemented in the EPS model.

4. DC-DC Converter design in LTspice

In this section we will describe the design of the DC-DC converters that will adapt the voltage delivered by the batteries to the modules according to the voltage level required by Table 2. These modules will behave as loads with a resistance and current consumption defined from their consumed power and operating voltage, relationship given by

$$R = \frac{V^2}{P} \qquad I = \frac{P}{V}$$

Table 3: Electrical parameters of the modules

Module	V (V)	Active P (W)	Active I (A)	Active R (Ω)	Idle P (W)	Idle I (A)	Idle R (Ω)
OBC	3.5	0.4	0.1143	30.63			
Payload	5	1.0	0.2000	25.00	0.500	0.1000	50.00
ADCS	5	1.2	0.2400	20.83	0.175	0.0350	142.86
TTEC	7.4	4.0	0.5405	13.69	0.480	0.0649	114.08

4.1. Boost Converter Sizing

The sizing of the converter consists of determining the parameters (duty cycle and switching frequency) and passive components (capacitor, inductor and resistor) that will produce the desired voltage level and good performance. As the resistor is the load of the module, it is not taken into account in the sizing, but the capacitance and inductor are.

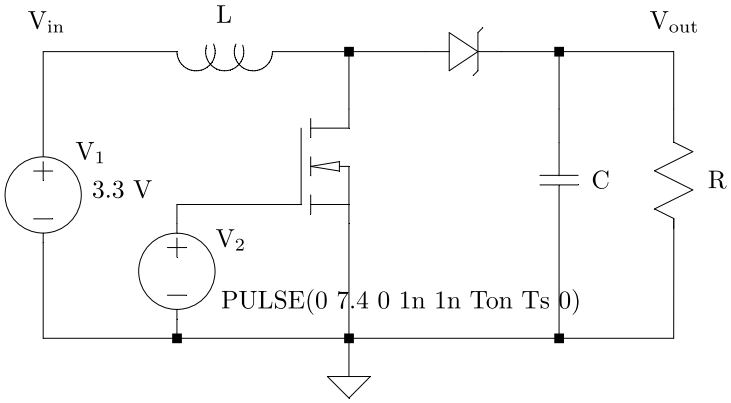

Figure 4: Boost Converter design.

4.1.1. Inductor sizing

Knowing the parameters of the converter, it is possible to determine the optimal and ideal value of L for the converter to work above the continuous and discontinuous driving limit, by means of the Equation (1).

$$L_{min} = \frac{D \cdot R \cdot (1 - D)^2}{2 \cdot f_s} \tag{1}$$

4.1.2. Capacitor sizing

In consequence to the output voltage power variations of the boost converter, a design criterion is used, which mentions that only a ripple voltage of up to 2% of the nominal output voltage should be allowed. Equation (2) represents a linear approximation of discharge of the output capacitor with a resistive load of R value, during the state in which the switch is in working position.

$$C_{min} = \frac{100 \cdot D \cdot T_s}{R} \tag{2}$$

Then with Equations (1) and (2) it is possible to calculate the minimum capacitance and inductance in the Boost converter design if used with the equivalent resistances of the modules given in the Table 3, this result together with the required duty cycle, and other parameters, are summarized in the following Table.

Table 4: Boost converter design parameters

	Vd (V)	Vo (V)	R (Ω)	D (%)	Ton (μs)	Cmin (μF)	Lmin (μH)
1	3.3	3.3	30.625	19.86	1.986	6.619	19.131
2	3.3	5.0	25.00	43.90	4.39	17.560	17.270
3	3.3	7.4	13.69	62.09	6.209	45.358	6.107

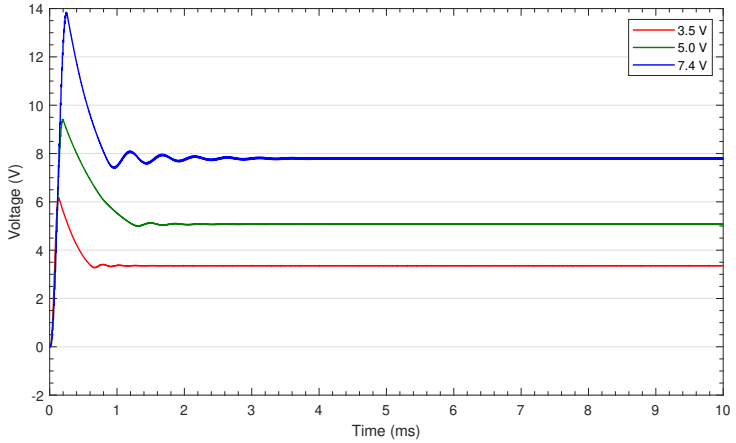

Figure 5: Converter voltage for 3 output voltages.

Table 5: Characteristic parameters of the theoretical design

	V_{avg}	T_r (μs)	OS (%)	T_s (ms)	r (%)	Eff (%)
1	3.352	41.00	84.67	0.63	0.41	74.92
2	5.072	61.40	85.64	1.10	0.47	81.97
3	7.796	81.13	77.65	1.62	0.86	89.95

4.2. Optimization by parameterization

The Equations (1) and (2) give us a whole set of values that, applied on pasive components, give us the desired voltage, but we can also optimize the voltage signal in terms of ripple, settling time, overshoot, and others. An optimization method has been proposed by [8, 9] where a variation of the RCL components of the converter circuit is performed in order to find the optimum values in the design. The effect of these components on the converter's performance, in terms of the voltage, can be seen in what we will call characteristic parameters, which include: rise time (Tr), overshoot percent (OS), settling time (Ts), ripple percent (r), and conversion efficiency (η). The effect of RCL values will affect one or more of these characteristic parameters, which will be analyzed to find the appropriate values for our EPS.

As a representative example, the parameterization of the Boost 3.3V to 5.5V converter corresponding to the Payload module is shown, starting from the design proposed in the previous section with the formulas used. In the parameterization of C and L values are swept around those chosen and greater than their minimum values obtained, C values are used between $20\,\mu F$ to $110\,\mu F$ with a step of $10\,\mu F$ and L values between $20\,\mu F$ to $200\,\mu F$ with a step of $10\,\mu F$. The resulting simulation will then give us the voltage V_{out} maintained by the converter for each case of C and L respectively, these are shown in the Figure 6b. Here it can be noted the dependence of some characteristic parameters on C or L, these can be deduced quantitatively if we extract the characteristic parameters from the voltage curves shown. In this case since the settling time and rise time are in the order of ms and μs, these parameters can be ignored. The parameters that are important in this analysis are overshoot, ripple, and efficiency; in varying C, no change in overshoot is observed, while increasing C there is a slight increase in efficiency and a better ripple is obtained (ripple decreases). Increasing L also shows a slight decrease in overshoot and an increase in efficiency while the ripple remains unchanged. From this we can deduce that overshoot depends only inversely on L, while ripple depends only inversely on C, and efficiency depends directly on both variables, with L being the most prominent.

It is clear that a high value of capacitance C generates a better response of the converter voltage, so a capacitor of $120\,\mu F$ is chosen, a value that maximizes efficiency and minimizes ripple. As for the inductor, the efficiency remains almost constant from $120\,\mu H$ while the overshoot decreases as L increases, an inductor of $150\,\mu H$ can be chosen.

The same process can be performed to the Boost converters corresponding to the OBC and TTEC module, where the parameterization values will depend on the one obtained in the sizing. The values chosen for the final design are a capacitance of $120\,\mu F$ for the three designs, while an inductance of $200\,\mu H$, $150\,\mu H$ and $10\,\mu H$ is obtained for the converters $3.5\,V$, $5.0\,V$ and $7.4\,V$ respectively. With the components selected the characteristic parameters of the new design take the values presented in the Table 6.

Table 6: Characteristic parameters of the final design

	V_{avg}	T_r (μs)	OS (%)	T_s (ms)	r (%)	Eff (%)
1	3.366	206.28	85.49	3.14	0.06	78.80
2	5.087	257.21	83.41	4.44	0.40	85.70
3	7.798	99.62	77.10	1.67	0.38	94.99

The main highlight of these results is the increase in efficiency achieved with the new parameters, reaching an increase between 4% and 5% of the values previously presented in the Table 5. It is also worth mentioning the change in the characteristic parameters, the most notorious is the increase in the rise and settling times, since those obtained are approximately 4 times larger; however, as mentioned, these are not relevant in the performance as long as they are maintained in an almost instantaneous time magnitude. As for the overshoot, no significant changes are obtained with the new parameters, while the ripple level is further decreased, which reproduces a finer voltage output.

It is also possible to perform a parameterization of R whose effects are mainly

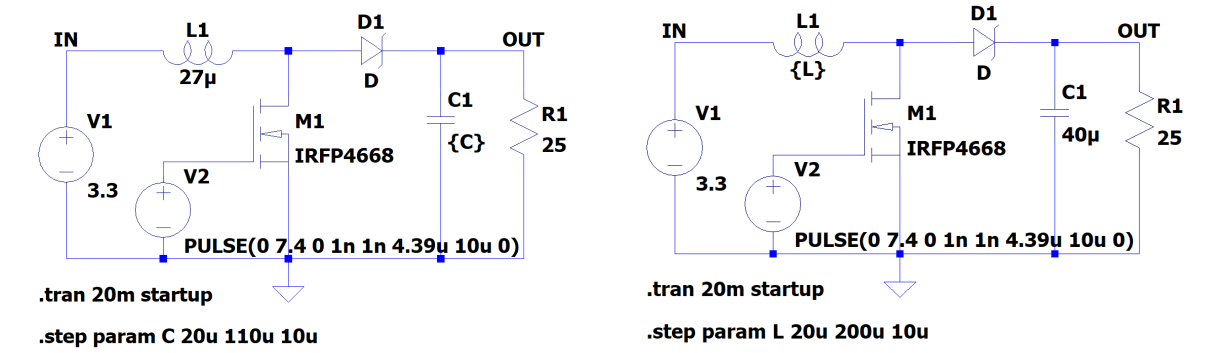

(a) LTspice designs for C and L parameterization.

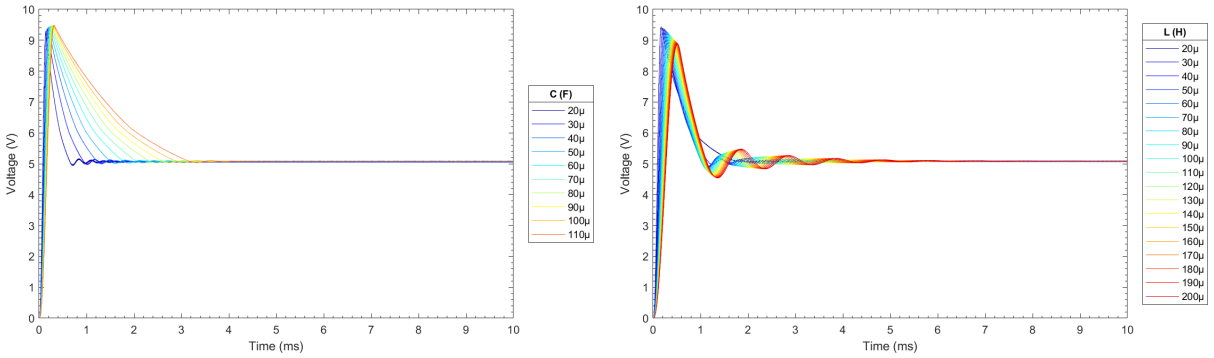

(b) C and L parameterization response voltages.

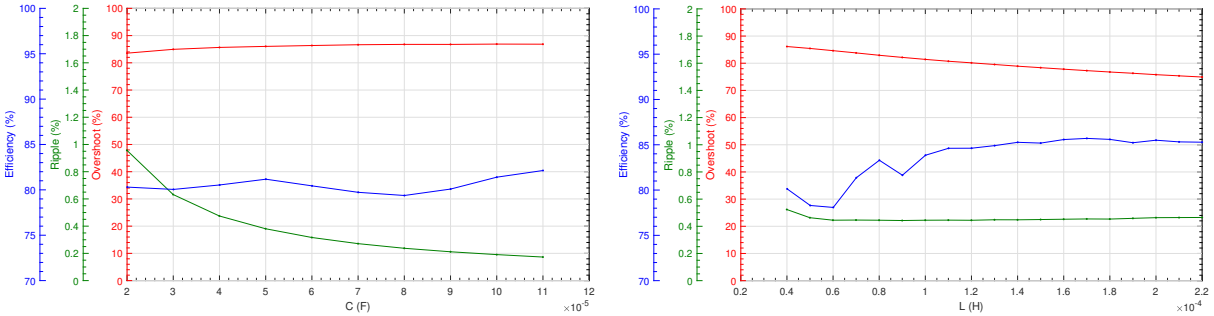

(c) Characteristic parameters of the parameterization of C and L.

Figure 6: Parameterization of capacitance C and inductance L in the Boost converter 3.3 V **to** 5.0 V**.**

manifested in the ripple and overshoot [8], but in this case such a process would be unnecessary in terms of converter design since the resistance is defined by the load according to the values presented in Table 3. However, the parameterization of R must be done to know the efficiency values at certain current consumptions, i.e., to obtain the efficiency curve of the DC-DC converter. For this purpose, the efficiency of the converter could be probed for a wide range of R values, but performing such a task in LTspice would be computationally expensive and perhaps unnecessary, so instead only the values of R that the model will require can be probed, such as the values presented in the Table 3.

5. EPS simulation results

Here we present the results related to the DC-DC converters designed in an EPS model in Simulink whose PCDU design is the one described in Figure 3, which includes three Boost converters $3.3\,\mathrm{V}$ to $3.5\,\mathrm{V}$, $5.0\,\mathrm{V}$ and $7.4\,\mathrm{V}$ which were characterized with the efficiency curve obtained from the parameterization in R, and with the 5 operational modes which indicate the state in which the EPS is operating. The output of the state diagram shows the transition between these modes, but the relevant ones for the converters are the safe mode and normal mode (any other mode) because when the safe mode is activated (SOC less than 40%) the Payload, the ADCS, and the usage time of the COM-TX module is reduced, this causes a lower power consumption and therefore another working point in the efficiency curve of the converter, when the safe mode is deactivated (SOC returns to 50%), it returns to the normal power consumption.

The Figure 7 shows the transition between the EPS operational modes and the efficiency values reached by each of the DC-DC converters. In the first $20\,\mathrm{h}$ it is observed that the modes oscillate in three types that present a normal power consumption, and after this time the safe mode is activated until almost $85\,\mathrm{h}$ of simulation. In all the time lapse we notice that the $3.5\,\mathrm{V}$ converter does not present any alteration because the OBC module works continuously regardless of the operating mode that is activated. On the other hand, in the first time lapse we observe fluctuations in the efficiency of the $5.0\,\mathrm{V}$ converter, this because the ADCS are maintained in a periodic operation as indicated in the Figure 2, while in the safe mode time lapse, where their corresponding modules (ADCS and Payload) are turned off, a uniform behavior is evidenced because the implemented efficiency curve does not consider the null consumptions (since it would imply an infinite resistance). Finally, it is observed that the $7.4\,\mathrm{V}$ converter presents an almost uniform efficiency, with periodic unevenness corresponding to the operation of the COM-TX module.

6. Conclusions

The proposed methodology for the design of a Boost converter starts from the sizing of its components C and L with Equations (1) y (2). From the resulting simulation in LTspice, the voltage maintained by the converter can be obtained as shown in the Figure 5, from which the characteristic parameters of this signal, such as overshoot, time constants, ripple, and efficiency, can be extracted. If required, it is possible to optimize the design by parameterizing C and L where its effect on the output voltage signal will be observed. By extracting the characteristic parameters of the voltage signals obtained from the parameterization we will have a quantitative result of this dependence, which is used to probe the values of C and L that make the converter response optimal, such as efficiency. If the values of C and L are properly chosen, we will obtain an optimal design of the converter, which will take advantage of the energy supplied by the EPS, improving its efficiency as presented in Table 6.

In addition, a parameterization is performed in R which is used only to get the efficiency curve as a function of the output current and which is implemented in the DC-DC converter blocks of Simulink. This last step is the most important since it allows to transfer the behavior of the converter designed in LTspice to the EPS model in Simulink by means of the efficiency curve.

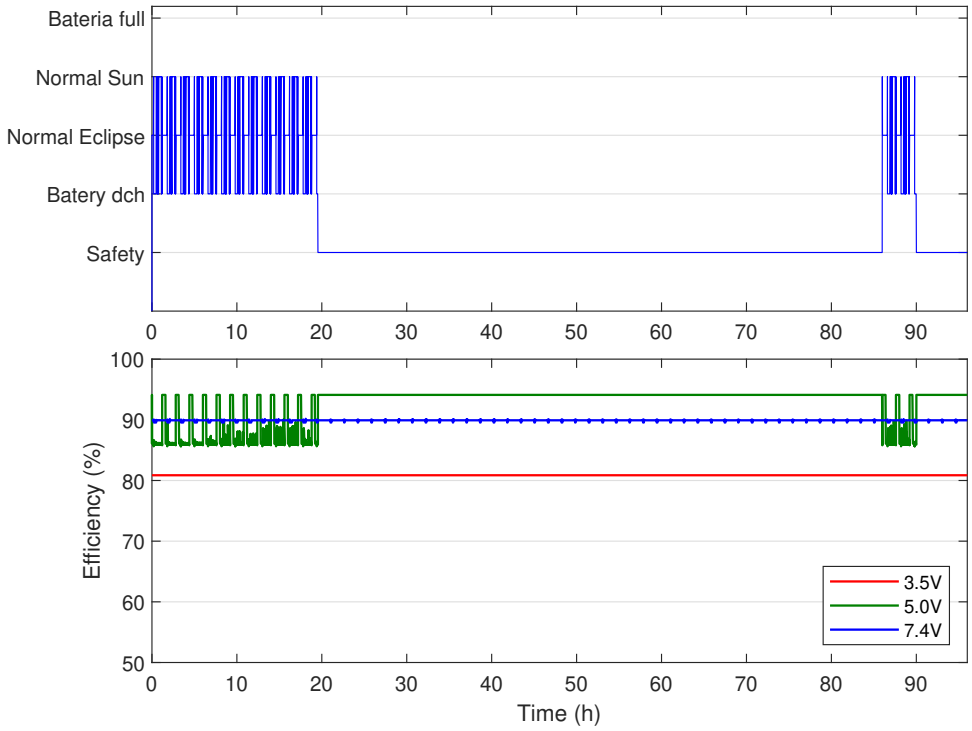

Figure 7: DC-DC converters efficiency during the simulation for 60P.

The parameterization process can also be employed if it is desired to decrease other parameters such as overshoot or even the time constants if they are taken into account in the analysis. In addition, the implementation of the efficiency curve in Simulink allows performing the simulation of the DC-DC converter for very large time periods, which would be unfeasible if the design is based on a switching frequency (originated by the MOSFET) due to the large difference in time scales.

References

[1] S. W. J. Puig-Suari, R. Coelho, The cubesat design specification rev. 12, CubeSat program, Cal. Poly SLO (2009).

[2] N. C. L. Initiative., Basic concepts and processes for first-time cubesat developers, https://www.nasa.gov/sites/default/files/atoms/files/nasa csli cubesat 101 508.pdf (2017).

[3] B. Yost, S. Weston, G. Benavides, F. Krage, J. Hines, S. Mauro, S. Etchey, K. O'Neill, B. Braun, State-of-the-art small spacecraft technology (2021).

[4] S. Acharya, F. Alshehhi, A. Tsoupos, O. Khan, M. Elmoursi, V. Khadkikar, H. Zeineldin, M. A. Hosani, Modeling and design of electrical power subsystem for cubesats, IEEE, 2019, pp. 1–6.

[5] A. Edpuganti, V. Khadkikar, M. S. Elmoursi, H. Zeineldin, M. A. Hosani, A novel eps architecture for 1u/2u cubesats with enhanced fault-tolerant capability, IEEE, 2020, pp. 1–6.

[6] A. Edpuganti, V. Khadkikar, H. Zeineldin, M. S. E. Moursi, M. A. Hosani, Comparison of peak power tracking based electric power system architectures for cubesats, IEEE Transactions on Industry Applications 57 (2021) 2758–2768.

[7] S. Sanchez-Sanjuan, J. Gonzalez-Llorente, R. Hurtado-Velasco, Comparison of the incident solar energy and battery storage in a 3u cubesat satellite for different orientation scenarios, Journal of Aerospace Technology and Management 8 (2016) 91–102.

[8] D. Naveda-Castillo, L. Adanaque-Infante, Characterization of dc converters for energy power systems on cubesats, in: 2020 IEEE XXVII International Conference on Electronics, Electrical Engineering and Computing (INTERCON), IEEE, pp. 1–4.

[9] J. D. G. Llorente, R. H. Velasco, S. A. S. Sanjuán, D. O. R. Duarte, A. J. R. Vecino, Obtención de energía solar y uso eficiente en la orientación de pequeños satélites, Fondo de publicaciones Universidad Sergio Arboleda, 2016.